Hindawi Publishing Corporation
Journal of Nanotechnology
Volume 2016, Article ID 6571643, 6 pages
http://dx.doi.org/10.1155/2016/6571643

Research Article

Synthesis and Magnetic Characterization of Graphite-Coated Iron Nanoparticles

A. M. Espinoza-Rivas,[1] M. A. Pérez-Guzmán,[2] R. Ortega-Amaya,[1] J. Santoyo-Salazar,[2,3] C. D. Gutiérrez-Lazos,[4] and M. Ortega-López[1,2]

[1]*Department of Electrical Engineering, Section of Solid State Electronics, Centro de Investigación y de Estudios Avanzados del Instituto Politécnico Nacional, Avenida IPN No. 2508, 07360 Ciudad de México, Mexico*
[2]*PhD Program in Nanoscience and Nanotechnology, Centro de Investigación y de Estudios Avanzados del Instituto Politécnico Nacional, Avenida IPN No. 2508, 07360 Ciudad de México, Mexico*
[3]*Departamento de Física, Centro de Investigación y de Estudios Avanzados del Instituto Politécnico Nacional, Avenida IPN No. 2508, 07360 Ciudad de México, Mexico*
[4]*Facultad de Ciencias Físico Matemáticas, Universidad Autónoma de Nuevo León, Avenida Universidad s/n, Ciudad Universitaria, 66455 San Nicolás de los Garza, NL, Mexico*

Correspondence should be addressed to M. Ortega-López; ortegal@cinvestav.mx

Received 16 February 2016; Accepted 11 April 2016

Academic Editor: Chuan Jian Zhong

Copyright © 2016 A. M. Espinoza-Rivas et al. This is an open access article distributed under the Creative Commons Attribution License, which permits unrestricted use, distribution, and reproduction in any medium, provided the original work is properly cited.

Graphite-coated iron nanoparticles were prepared from magnetite nanoparticles by chemical vapour deposition (CVD) under methane and hydrogen atmosphere. After being purified from carbon excess, graphite-coated iron nanoparticles were tested for morphological and magnetic properties. It was found that, during the thermal process, magnetite nanoparticles 6 nm in size coalesce and transform into graphite-coated iron 200 nm in size, as revealed by scanning electron microscopy (SEM). Raman characterization assessed that high-quality graphite coats the iron core. Magnetic measurements revealed the phase change (magnetite to iron) as an increase in the saturation magnetization from 50 to 165 emu/g after the CVD process.

1. Introduction

Currently there exists the interest in the synthesis and characterization of magnetic nanomaterials because of their multiple applications such as magnetic storage [1, 2], spintronics [3], hyperthermia [4], cell labelling [5], drug delivery [6], magnetic resonance imaging (MRI) contrast enhancement [7, 8], and magnetically assisted chemotherapy [9–11]. Among the different magnetic materials, magnetite (Fe_3O_4) has been intensively studied for the abovementioned applications.

For many applications the physicochemical stability of the nanoparticle is an important issue [12]. Because of their chemical activity, nanosized materials easily interact with undesirable molecular species to undergo degradation which means a drawback for some applications [13]. Several approaches have been addressed to overcome the stabilization problem, mostly including the organic passivation of the surface nanoparticle [14]. In the magnetite nanoparticles case, oleic acid has proven to be an excellent stabilizing agent to prevent its chemical degradation [15]. Organic compounds other than oleic acid such as citric acid and polylactic acid [16–18] have also successfully used to stabilize and disperse magnetic nanoparticles in aqueous or organic medium [19, 20].

In addition to organic molecules, inorganic coatings have successfully been tested as the stabilizing shell of magnetic nanoparticles with inorganic materials; two common examples of inorganic shells are silica [21] and gold [22]. In spite of being a biocompatible material and providing a multifunctional platform for surface modification, it was reported that gold shells fail to protect magnetic nanoparticles [23] because

they usually have grain boundaries. Therefore, new materials for making more stable and hermetic shells are demanded.

On the other hand, iron nanoparticles are currently studied for environmental remediation and hyperthermia [24]. For instance, graphite-coated iron nanoparticles were used to remove heavy metal ions (Cu^{2+}, Co^{2+}, and Cd^{2+}) from water [25], uranium [26], and arsenic [27] or Co^{2+} ions from an effluent [28]. In addition, graphite has proven to be an excellent coating to protect the magnetic iron core from physicochemical degradation under corrosive medium [29].

Carbon-coated iron nanoparticles have been produced by different methods including detonation-induced pyrolysis of ferrocene [30], arc-discharge [31], pulsed laser irradiation [32], and CVD [33].

In this paper, we report the synthesis and the structural and magnetic characterization of graphite-coated iron nanoparticles. These particles were obtained from our experiments tending to hermetically coat magnetite nanoparticles with a graphite coating by CVD, CVD being a suitable method to form hard graphite coatings on a variety of metal surfaces. The subsequent characterization indicated that graphite-coated nanoparticles could be obtained, but magnetite transformed into elemental iron due to the reductive atmosphere and methane inside the CVD reactor. Importantly, the prepared particles demonstrated long term stability against oxidation under environmental conditions.

2. Materials and Methods

2.1. Sample Preparation. The graphite-coated iron nanoparticles were produced by CVD using magnetite nanoparticles as the starting material.

The magnetite nanoparticles (MNPs) were prepared by coprecipitation of $FeCl_2$ and $FeCl_3$ salts in water using NH_4OH as precipitant [34]. The obtained product was thoroughly magnetically assisted water-washed to purify it from byproducts and then dried to obtain a powder comprising magnetite nanoparticles 6 nm in size exhibiting superparamagnetism.

For the CVD process, the as-prepared magnetite nanoparticles powder was placed on a copper foil and introduced in the tube quartz of a homemade CVD system.

The CVD process started by establishing an argon flow (424 sccm) while the temperature was raised up to 800°C and kept so for 30 min. Afterward, a hydrogen flow (420 sccm) was turned on and the argon flow was turned off while the temperature was raised to 900°C. After 30 min a methane flow (50 sccm) was added and it is kept for 30 min maintaining the hydrogen flow for additional 30 min.

2.2. Characterization Techniques. The obtained material was characterized by transmission electron microscopy (TEM) (JEOL 2010), high resolution transmission electron microscopy (TEM) (JEM-ARM200F), scanning electron microscopy (SEM) (Zeiss Auriga), vibrating sample magnetometry (VSM) (Lake Shore 7300), X-ray diffraction XRD (X'pert Pro) using Cu k_α radiation, and Raman spectroscopy (Horiba Jobin-Yvon) 532 nm laser line.

3. Results and Discussion

3.1. Phase Composition and Morphology

3.1.1. Morphology. As previously established, the graphite-coated iron nanoparticles (GFeNps) were prepared from magnetite powders comprising particles 6 nm in size. Magnetization experiments indicated that the magnetite sample displays a superparamagnetic behaviour with 50 emu/g saturation magnetization.

After the thermal process, iron-based nanophases other than magnetite developed, depending on the existent atmosphere in the CVD reactor. Under the methane-hydrogen atmosphere, single phase iron nanoparticles along with some carbon-derived nanostructures (graphene sheets, highly oriented graphite, and nanotubes) were obtained. Carbon nanostructures were removed by crushing the as-prepared material in a mortar followed by magnetic separation. As shown in the scanning electron microscopy (SEM) images (Figure 1(a)), the obtained sample consists of core-shell graphite-iron particles 300 and 500 nm in size as the main product. The core-shelled structure for the obtained iron nanoparticles was assessed by HRTEM; Figure 1(b) shows TEM of GFeNps.

3.1.2. Phase Composition

X-Ray Diffraction Characterization. Figure 2 shows the XRD spectra of magnetite nanoparticles (JPCDS-PDF-19-0629) (b) and graphite-encapsulated iron nanoparticles (a). All of the peaks appearing in the CVD treated samples belong to the BCC phase of iron (JPCDS-PDF-6-0696) [35] indicating that magnetite completely transforms into elemental iron. A small peak corresponding to the graphitic material (JPCDS-PDF-56-0159) is also present. If present, iron carbide phases were undetectable for X-ray diffraction.

The crystallite size, as calculated from XRD data using the Scherrer equation, was 11 nm and 23 nm for magnetite and graphite-coated iron, respectively.

Raman Spectroscopy Characterization. Graphitic materials display the D (1350 cm^{-1}), G (1580 cm^{-1}), and G′ (2700 cm^{-1}) typical bands in their Raman spectrum, which are ascribed to defects in the crystalline structure, the characteristic sigma bond between two hybrid orbitals sp^2, and the characteristic overtone of the D band [36–38], respectively. In the present case, the representative Raman spectrum of our samples (Figure 3) clearly indicates the high quality for the iron nanoparticle graphite coating, because it resembles to that reported for highly oriented graphite [39, 40].

Proposed Formation Mechanism for GFeNps. The above results indicate that graphite-coated iron nanoparticles could be obtained under the previously described experimental conditions. To explain the whole process leading to the GFeNps formation and the graphite coating development (Figure 4), it is noteworthy to mention that preliminary studies on Ar annealed magnetite nanoparticles at 800°C indicated no phase change in the starting material. Hence, we

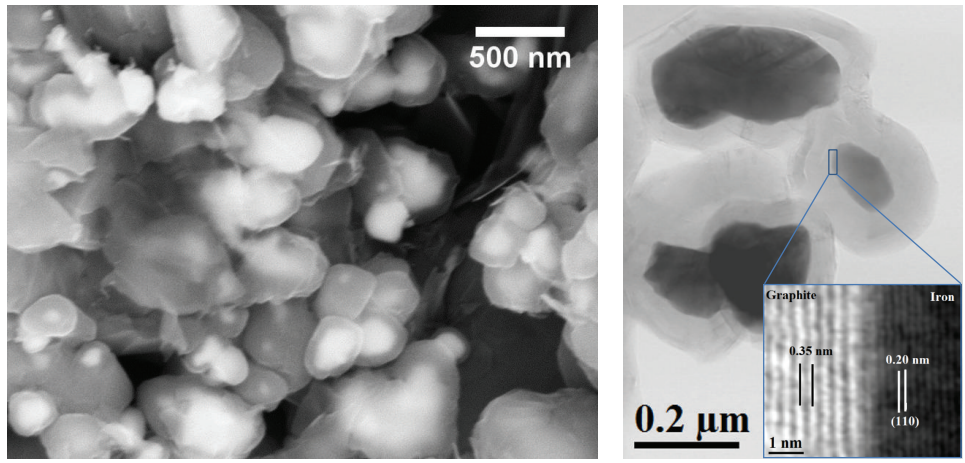

Figure 1: (a) SEM image of a GFeNps sample as obtained from the CVD process and (b) HRTEM image of a GFeNp. The inset shows details on the GFeNps core-shell structure. Note that 0.35 nm and 0.206 nm agree well with the interplanar separation of graphite layers and (110) planes of Fe, respectively.

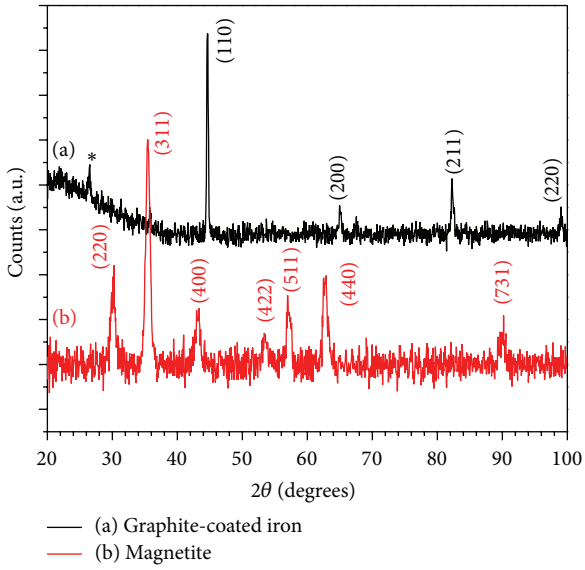

Figure 2: X-ray diffraction of graphite-encapsulated iron nanoparticles (a) and bare magnetite (b); the peak marked by ∗ corresponds to the plane (002) of graphite.

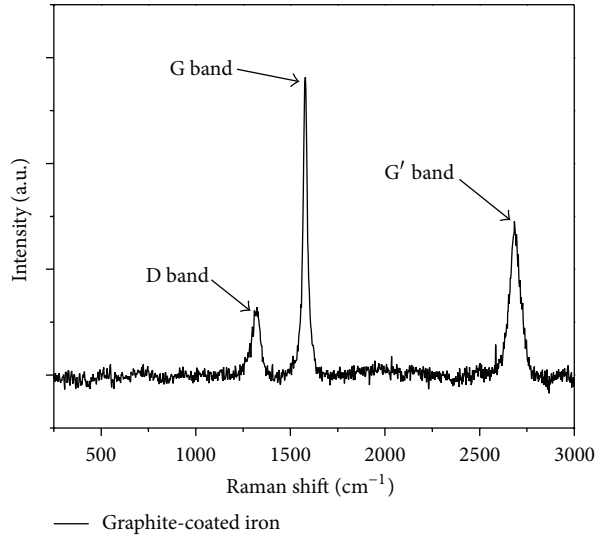

Figure 3: Raman spectrum of graphite-encapsulated iron nanoparticles.

have assumed that both the transformation of magnetite to elemental iron and the graphite coating development occur at 900°C in presence of the methane-hydrogen mixture. At first, the MNPs 6 nm in size agglomerate and then coalesce to develop larger polycrystalline magnetite nanoparticles at 800°C under Ar atmosphere. Upon establishing the hydrogen-methane atmosphere at 900°C, carbon and carbon hydride species are produced and then react with iron oxide to reduce it into elemental iron. At 900°C, the nanoparticle surface is partially melted and the magnetite oxygen reacts with carbon and carbon hydride species to produce elemental iron. The complete transformation of magnetite into iron involves oxygen exodiffusion from the nanoparticle volume.

In regard to the graphite coating development, we believe that it grows following a genuine CVD process. That is, because of the catalytic action of iron widely observed [41] the hydrogenated carbon species catalytically decompose into carbon atoms (black dots in Figure 4) at the partially melted surface of the iron nanoparticle, and then carbon atoms react with iron to form a carbon-rich iron surface. After reaching the carbon supersaturation, graphene nucleates at the grain boundaries and then it conformally grows to completely coat the particle surface. The subsequent graphene overlayers develop on the underneath one through an autocatalytic mechanism involving structural defects in the graphene

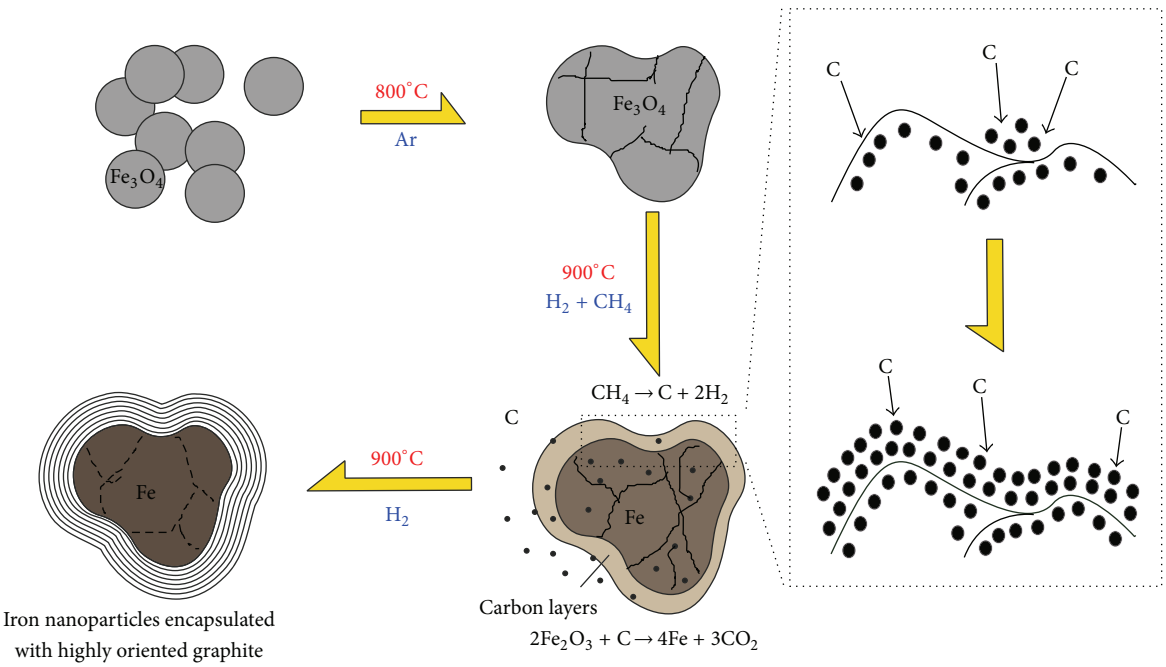

FIGURE 4: Assumed development of GFeNps: At 800°C, smaller magnetite nanoparticles coalesce into a larger polycrystalline one under Ar atmosphere. At 900°C, hydrogen reacts with methane to produce carbon and carbon-hydrogen derived species, which impinge on the partially melted iron surface to form a thin carbon-rich iron surface. After reaching the carbon supersaturation, graphene nucleates at the grain boundaries and then it conformally grows to completely coat the particle surface.

structure. Figure 4 schematizes the proposed formation mechanism for GFeNps. Previous studies have reported similar structures where the graphitization occurred at the big nanoparticles surface, so forming highly oriented graphite which is represented and excellent protection against the oxidation of the magnetic core [42, 43].

3.1.3. Magnetic Characterization. As previously mentioned, the CVD process promotes the iron-oxide-to-elemental-iron conversion. Figure 5 shows the magnetization curves of the material before (a) and after (b) the CVD process. The magnetization curve of MNPs (magnetite) assesses its superparamagnetic character, with saturation magnetization M_s = 50 emu/g, which agrees well with that reported for magnetite nanoparticles 6 nm in size [44].

On the other hand, the graphite-coated iron nanoparticles saturation magnetization curve indicates that they are nearly superparamagnetic ones, with coercivity of 17 Oe and M_s = 165 emu/g. The superparamagnetic deviation is probably due to the polydisperse nature of the sample. The increment of M_s represents 3.3 times the value of the original particles. These striking changes corroborate the notion that magnetite transforms into elemental iron [45], because the measured M_s value agrees well with that reported for iron nanoparticles (M_s = 178 emu/g) [46].

The superparamagnetic character of magnetite was assessed by fitting the magnetization experimental data to the Langevin equation as proposed by Knobel et al. [47] and Goya et al. [48] (see Figure 6). For this, the log-normal distribution function was used and a spherical shape

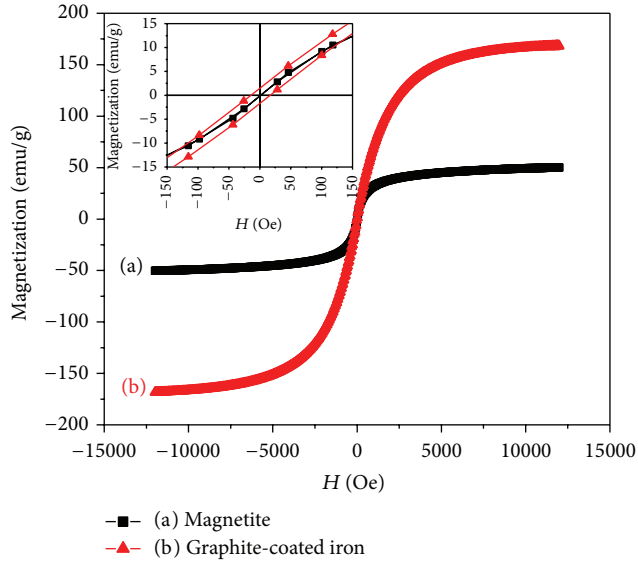

FIGURE 5: Magnetization curves at room temperature: magnetite nanoparticles (a) and graphite-coated iron nanoparticles (b). The inset displays the low field magnetization to illustrate the superparamagnetic nature of our samples.

for the magnetite nanoparticles was assumed. The relevant parameters obtained from the fitting procedure were the distribution median μ_0 = 1705 μ_B, standard deviation σ = 1.24, and mean magnetic moment μ_m = 3678 μ_B, μ_B being the Bohr magneton. It is noteworthy that the μ_m value agrees

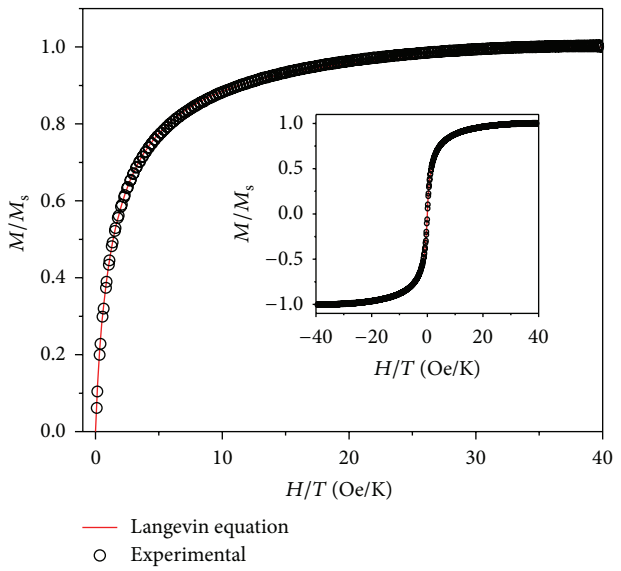

FIGURE 6: Normalized magnetization curve of magnetite (○) fitted with a Langevin function (solid line); the used parameters were $\mu_0 = 1705\,\mu_B$, $T = 300$ K, and $\sigma = 1.24$.

fairly well with the magnetic moment for a 6 nm SPION, as estimated by considering $32\,\mu_B$ per magnetite unit cell and counting the unit cell number per particle. This suggests that the magnetite sample comprises monodomain nanoparticles.

4. Conclusions

We reported the preparation and magnetic properties and structural and morphological characterization of graphite-coated iron nanoparticles, which were obtained from CVD-processed magnetite nanoparticles. The XRD studies indicated the complete transformation of magnetite to iron and the graphite presence. The magnetic characterization revealed a nearly superparamagnetic behaviour for the graphite-coated iron nanoparticles. The relative low coercive field of our sample was attributed to its polydisperse character, which was caused by the process to encapsulate magnetic nanoparticles with graphite using the CVD technique. The Raman spectrum assessed the high quality of the graphitic material coating the iron nanoparticles.

Competing Interests

The authors declare that they have no competing interests.

Acknowledgments

This work was supported by the Consejo Nacional de Ciencia y Tecnología (CONACyT) scholarships. The authors are grateful to Alvaro Guzman Campuzano for their invaluable help in the experimental work, to the Laboratorio Avanzado de Nanoscopía Electrónica (LANE-CINVESTAV) facilities, and especially to Josue Romero Ibarra for the SEM images.

References

[1] G. Reiss and A. Hütten, "Magnetic nanoparticles: applications beyond data storage," *Nature Materials*, vol. 4, no. 10, pp. 725–726, 2005.

[2] P. Tartaj, M. P. Morales, T. Gonzalez-Carreño, S. Veintemillas-Verdaguer, and C. J. Serna, "The iron oxides strike back: from biomedical applications to energy storage devices and photoelectrochemical water splitting," *Advanced Materials*, vol. 23, no. 44, pp. 5243–5249, 2011.

[3] S. Hihath, R. A. Kiehl, and K. V. Benthem, "Interface composition between Fe_3O_4 nanoparticles and GaAs for spintronic applications," *Journal of Applied Physics*, vol. 116, no. 8, Article ID 084306, 2014.

[4] M. Vasilakaki, C. Binns, and K. N. Trohidou, "Susceptibility losses in heating of magnetic core/shell nanoparticles for hyperthermia: a Monte Carlo study of shape and size effects," *Nanoscale*, vol. 7, no. 17, pp. 7753–7762, 2015.

[5] M. P. Calatayud, B. Sanz, V. Raffa, C. Riggio, M. R. Ibarra, and G. F. Goya, "The effect of surface charge of functionalized Fe_3O_4 nanoparticles on protein adsorption and cell uptake," *Biomaterials*, vol. 35, no. 24, pp. 6389–6399, 2014.

[6] W. Gao and J. Wang, "Synthetic micro/nanomotors in drug delivery," *Nanoscale*, vol. 6, no. 18, pp. 10486–10494, 2014.

[7] K. Ohno, C. Mori, T. Akashi et al., "Fabrication of contrast agents for magnetic resonance imaging from polymer-brush-afforded iron oxide magnetic nanoparticles prepared by surface-initiated living radical polymerization," *Biomacromolecules*, vol. 14, no. 10, pp. 3453–3462, 2013.

[8] S. A. Corr, S. J. Byrne, R. Tekoriute et al., "Linear assemblies of magnetic nanoparticles as MRI contrast agents," *Journal of the American Chemical Society*, vol. 130, no. 13, pp. 4214–4215, 2008.

[9] Q. A. Pankhurst, J. Connolly, S. K. Jones, and J. Dobson, "Applications of magnetic nanoparticles in biomedicine," *Journal of Physics D: Applied Physics*, vol. 36, no. 13, article R167, 2003.

[10] M. Mahmoudi, S. Sant, B. Wang, S. Laurent, and T. Sen, "Superparamagnetic iron oxide nanoparticles (SPIONs): development, surface modification and applications in chemotherapy," *Advanced Drug Delivery Reviews*, vol. 63, no. 1-2, pp. 24–46, 2011.

[11] C. H. Cunningham, T. Arai, P. C. Yang, M. V. McConnell, J. M. Pauly, and S. M. Conolly, "Positive contrast magnetic resonance imaging of cells labeled with magnetic nanoparticles," *Magnetic Resonance in Medicine*, vol. 53, no. 5, pp. 999–1005, 2005.

[12] A.-H. Lu, E. L. Salabas, and F. Schüth, "Magnetic nanoparticles: synthesis, protection, functionalization," *Angewandte Chemie—International Edition*, vol. 46, no. 8, pp. 1222–1244, 2007.

[13] A. Akbarzadeh, M. Samiei, and S. Davaran, "Magnetic nanoparticles: preparation, physical properties, and applications in biomedicine," *Nanoscale Research Letters*, vol. 7, article 144, 2012.

[14] V. K. Sharma, K. M. Siskova, R. Zboril, and J. L. Gardea-Torresdey, "Organic-coated silver nanoparticles in biological and environmental conditions: fate, stability and toxicity," *Advances in Colloid and Interface Science*, vol. 204, pp. 15–34, 2014.

[15] C. Rodríguez, M. Bañobre-López, Y. V. Kolen'Ko, B. Rodríguez, P. Freitas, and J. Rivas, "Magnetization drop at high temperature in oleic acid-coated magnetite nanoparticles," *IEEE Transactions on Magnetics*, vol. 48, no. 11, pp. 3307–3310, 2012.

[16] M. E. de Sousa, M. B. Fernández Van Raap, P. C. Rivas et al., "Stability and relaxation mechanisms of citric acid coated

magnetite nanoparticles for magnetic hyperthermia," *Journal of Physical Chemistry C*, vol. 117, no. 10, pp. 5436–5445, 2013.

[17] S. A. Gómez-Lopera, J. L. Arias, V. Gallardo, and A. V. Delgado, "Colloidal stability of magnetite/poly(lactic acid) core/shell nanoparticles," *Langmuir*, vol. 22, no. 6, pp. 2816–2821, 2006.

[18] S. Khoee and A. Kavand, "A new procedure for preparation of polyethylene glycol-grafted magnetic iron oxide nanoparticles," *Journal of Nanostructure in Chemistry*, vol. 4, no. 3, pp. 1–6, 2014.

[19] T. Kikuchi, R. Kasuya, S. Endo et al., "Preparation of magnetite aqueous dispersion for magnetic fluid hyperthermia," *Journal of Magnetism and Magnetic Materials*, vol. 323, no. 10, pp. 1216–1222, 2011.

[20] C. Sciancalepore, R. Rosa, G. Barrera, P. Tiberto, P. Allia, and F. Bondioli, "Microwave-assisted nonaqueous sol-gel synthesis of highly crystalline magnetite nanocrystals," *Materials Chemistry and Physics*, vol. 148, no. 1-2, pp. 117–124, 2014.

[21] X. Ni, Z. Zheng, X. Xiao, L. Huang, and L. He, "Silica-coated iron nanoparticles: shape-controlled synthesis, magnetism and microwave absorption properties," *Materials Chemistry and Physics*, vol. 120, no. 1, pp. 206–212, 2010.

[22] S.-J. Cho, J.-C. Idrobo, J. Olamit, K. Liu, N. D. Browning, and S. M. Kauzlarich, "Growth mechanisms and oxidation resistance of gold-coated iron nanoparticles," *Chemistry of Materials*, vol. 17, no. 12, pp. 3181–3186, 2005.

[23] B. Ravel, E. E. Carpenter, and V. G. Harris, "Oxidation of iron in iron/gold core/shell nanoparticles," *Journal of Applied Physics*, vol. 91, article 8195, 2002.

[24] A. Taylor, Y. Krupskaya, K. Krämer et al., "Cisplatin-loaded carbon-encapsulated iron nanoparticles and their in vitro effects in magnetic fluid hyperthermia," *Carbon*, vol. 48, no. 8, pp. 2327–2334, 2010.

[25] M. Bystrzejewski, K. Pyrzyńska, A. Huczko, and H. Lange, "Carbon-encapsulated magnetic nanoparticles as separable and mobile sorbents of heavy metal ions from aqueous solutions," *Carbon*, vol. 47, no. 4, pp. 1201–1204, 2009.

[26] M. Dickinson and T. B. Scott, "The application of zero-valent iron nanoparticles for the remediation of a uranium-contaminated waste effluent," *Journal of Hazardous Materials*, vol. 178, no. 1–3, pp. 171–179, 2010.

[27] S. R. Kanel, D. Nepal, B. Manning, and H. Choi, "Transport of surface-modified iron nanoparticle in porous media and application to arsenic(III) remediation," *Journal of Nanoparticle Research*, vol. 9, no. 5, pp. 725–735, 2007.

[28] Ç. Üzüm, T. Shahwan, A. E. Eroğlu, I. Lieberwirth, T. B. Scott, and K. R. Hallam, "Application of zero-valent iron nanoparticles for the removal of aqueous Co^{2+} ions under various experimental conditions," *Chemical Engineering Journal*, vol. 144, no. 2, pp. 213–220, 2008.

[29] D. Zhang, S. Wei, C. Kaila et al., "Carbon-stabilized iron nanoparticles for environmental remediation," *Nanoscale*, vol. 2, no. 6, pp. 917–919, 2010.

[30] Y. Lu, Z. Zhu, and Z. Liu, "Carbon-encapsulated Fe nanoparticles from detonation-induced pyrolysis of ferrocene," *Carbon*, vol. 43, no. 2, pp. 369–374, 2005.

[31] P.-Z. Si, Z.-D. Zhang, D.-Y. Geng, C.-Y. You, X.-G. Zhao, and W.-S. Zhang, "Synthesis and characteristics of carbon-coated iron and nickel nanocapsules produced by arc discharge in ethanol vapor," *Carbon*, vol. 41, no. 2, pp. 247–251, 2003.

[32] J. B. Park, S. H. Jeong, M. S. Jeong, J. Y. Kim, and B. K. Cho, "Synthesis of carbon-encapsulated magnetic nanoparticles by pulsed laser irradiation of solution," *Carbon*, vol. 46, no. 11, pp. 1369–1377, 2008.

[33] H. Cao, G. Huang, S. Xuan, Q. Wu, F. Gu, and C. Li, "Synthesis and characterization of carbon-coated iron core/shell nanostructures," *Journal of Alloys and Compounds*, vol. 448, no. 1-2, pp. 272–276, 2008.

[34] M. A. Pérez-Guzmán, *Sintesis, funcionalización y caracterizacion de nanoparticulas superparamagneticas de magnetita [M.S. thesis]*, Departamento de Ingenieria Electrica, CINVESTAV-IPN, Mexico City, Mexico, 2013.

[35] J. Cui, H. Zhang, L. Chen, H. Li, and W. Tong, "Microstructure and mechanical properties of a wear-resistant as-cast alloyed bainite ductile iron," *Acta Metallurgica Sinica*, vol. 27, no. 3, pp. 476–482, 2014.

[36] F. Tuinstra and J. L. Koenig, "Raman spectrum of graphite," *The Journal of Chemical Physics*, vol. 53, no. 3, pp. 1126–1130, 1970.

[37] F. Negri, E. Di Donato, M. Tommasini, C. Castiglioni, G. Zerbi, and K. Müllen, "Resonance Raman contribution to the D band of carbon materials: modeling defects with quantum chemistry," *Journal of Chemical Physics*, vol. 120, Article ID 11889, 2004.

[38] S. Reich and C. Thomsen, "Raman spectroscopy of graphite," *Philosophical Transactions of the Royal Society A: Mathematical, Physical and Engineering Sciences*, vol. 362, no. 1824, pp. 2271–2288, 2004.

[39] P. Tan, Y. Deng, and Q. Zhao, "Temperature-dependent Raman spectra and anomalous Raman phenomenon of highly oriented pyrolytic graphite," *Physical Review B*, vol. 58, no. 9, pp. 5435–5439, 1998.

[40] T. Jawhari, A. Roid, and J. Casado, "Raman spectroscopic characterization of some commercially available carbon black materials," *Carbon*, vol. 33, no. 11, pp. 1561–1565, 1995.

[41] Y. Gao, G. P. Pandey, J. Turner, C. R. Westgate, and B. Sammakia, "Chemical vapor-deposited carbon nanofibers on carbon fabric for supercapacitor electrode applications," *Nanoscale Research Letters*, vol. 7, article 651, 2012.

[42] M. R. Sanaee and E. Bertran, "Synthesis of carbon encapsulated mono- and multi-iron nanoparticles," *Journal of Nanomaterials*, vol. 2015, Article ID 450183, 10 pages, 2015.

[43] E. Ye, B. Liu, and W. Y. Fan, "Preparation of graphite-coated iron nanoparticles using pulsed laser decomposition of $Fe_3(CO)_{12}$ and PPh_3 in hexane," *Chemistry of Materials*, vol. 19, no. 15, pp. 3845–3849, 2007.

[44] K. Abdulwahab, M. A. Malik, P. O'Brien et al., "Synthesis of monodispersed magnetite nanoparticles from iron pivalate clusters," *Dalton Transactions*, vol. 42, no. 1, pp. 196–206, 2013.

[45] J. Mendez-Garza, B. Wang, A. Madeira, C. D. Giorgio, and G. Bossis, "Synthesis and surface modification of spindle-type magnetic nanoparticles: gold coating and peg functionalization," *Journal of Biomaterials and Nanobiotechnology*, vol. 4, no. 3, pp. 222–228, 2013.

[46] D. L. Huber, "Synthesis, properties, and applications of iron nanoparticles," *Small*, vol. 1, no. 5, pp. 482–501, 2005.

[47] M. Knobel, W. C. Nunes, L. M. Socolovsky, E. De Biasi, J. M. Vargas, and J. C. Denardin, "Superparamagnetism and other magnetic features in granular materials: a review on ideal and real systems," *Journal of Nanoscience and Nanotechnology*, vol. 8, no. 6, pp. 2836–2857, 2008.

[48] G. F. Goya, T. S. Berquó, F. C. Fonseca, and M. P. Morales, "Static and dynamic magnetic properties of spherical magnetite nanoparticles," *Journal of Applied Physics*, vol. 94, no. 5, pp. 3520–3528, 2003.


Journal of
Nanotechnology

International Journal of
Corrosion

International Journal of
Polymer Science

Smart Materials
Research

Journal of
Composites

BioMed
Research International
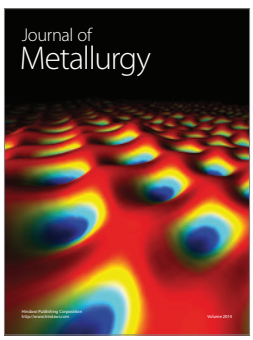
Journal of
Metallurgy

Journal of
Materials

Hindawi
Submit your manuscripts at
http://www.hindawi.com
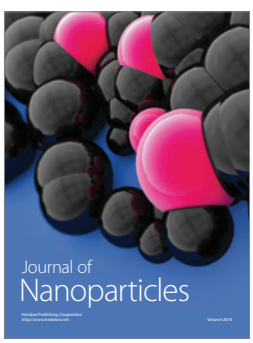
Journal of
Nanoparticles
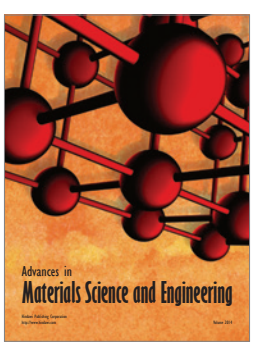
Advances in
Materials Science and Engineering
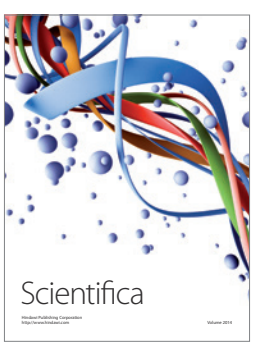
Scientifica
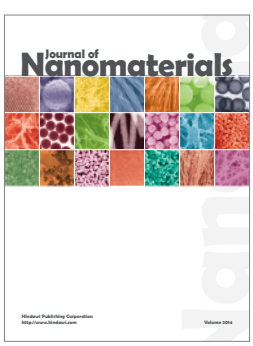
Journal of
Nanomaterials

The Scientific
World Journal

International Journal of
Biomaterials
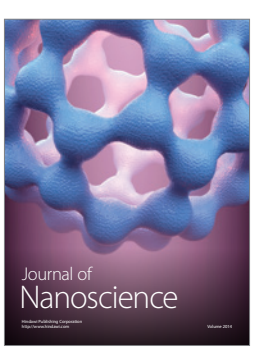
Journal of
Nanoscience

Journal of
Coatings
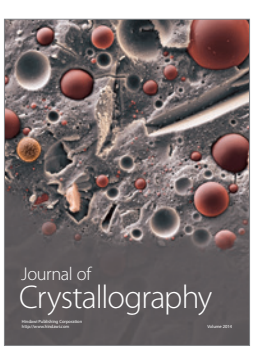
Journal of
Crystallography

Journal of
Ceramics
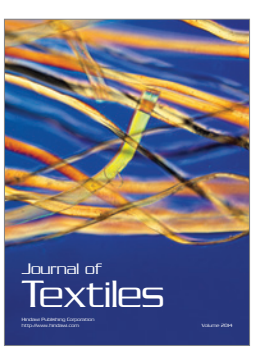
Journal of
Textiles